Regioreversed Thermal and Photochemical Reduction of 10-Methylacridinium and 1-Methylquinolinium Ions by Organosilanes and Oraganostannanes

Shunichi Fukuzumi,*,† Morifumi Fujita,†,‡ Souta Noura,† Kei Ohkubo,† Tomoyoshi Suenobu,† Yasuyuki Araki,§ and Osamu Ito§

Department of Material and Life Science, Graduate School of Engineering, Osaka University, CREST, Japan Science and Technology Corporation (JST), Suita, Osaka 565-0871, Japan, and Institute for Chemical Reaction Science, Tohoku University, CREST, Japan Science and Technology Corporation (JST), Sendai, Miyagi 980-8577, Japan

Received: September 27, 2000; In Final Form: December 18, 2000

Irradiation of the absorption band of the 10-methylacridinium ion ($AcrH^+$) in acetonitrile containing allylic silanes and stannanes results in the efficient and selective reduction of the 10-methylacridinium ion to yield the allylated dihydroacridines. In the photochemical reactions of $AcrH^+$ with unsymmetric allylsilanes, the allylic groups are introduced selectively at the α position. Likewise, the reactions with unsymmetric allylstannanes afforded the α adducts predominantly, but the γ adducts were also obtained as minor products. In contrast to this, the thermal reduction of $AcrH^+$ and the 1-methylquinolinium ion (QuH^+) by unsymmetric allylstannanes gave only the γ adducts. The thermal reduction of QuH^+ by tributyltin hydride or hydrosilanes in the presence of a fluoride anion also occurs to yield 1-methyl-1,2-dihydroquinoline selectively. On the other hand, the photoreduction of QuH^+ derivatives by tributyltin hydride and tris(trimethylsilyl)silane yields the corresponding 1,4-dihydroquinolines exclusively. The difference in the mechanisms for the regioreversed thermal and photochemical reduction of $AcrH^+$ and QuH^+ is discussed in terms of nucleophilic vs electron-transfer pathways. The photochemical reactions proceed via photoinduced electron transfer from organosilanes and organostannanes to the singlet excited states of $AcrH^+$ and QuH^+, followed by the radical coupling of the resulting radical pair in competition with the back electron transfer to the ground state. The rate constants of photoinduced electron transfer obtained from the fluorescence quenching of $AcrH^+$ and QuH^+ by organosilane and organostannane donors agree with those obtained from the dependence of the quantum yields on the donor concentrations for the photochemical reactions. The electron-transfer rate constants are well analyzed in light of the Marcus theory of adiabatic outer-sphere electron transfer, leading to the evaluation of the reorganization energy ($\lambda = 0.90$ eV) of the electron-transfer reactions. The transient spectra of the radical pair produced by the photoinduced electron transfer from organosilanes to the singlet excited state of $AcrH^+$ have been successfully detected in laser-flash photolysis of the $AcrH^+$−organosilane systems. The rate constants of back electron transfer to the ground state have been determined, leading to the evaluation of the reorganization energy for the back electron transfer, which agrees with the value for the forward electron transfer.

Introduction

The carbon−carbon bond formation via photoinduced electron-transfer reactions of organosilanes and organostannanes has attracted growing interest not only because of the mechanistic aspects but also in view of their synthetic utility.[1−6] A pioneering work by Mariano and co-workers[1,2] has demonstrated that desilylation processes from organosilanes attendant upon the photoinduced electron-transfer oxidation constitute effective methods for site-selective generation of organic radicals which can serve as intermediates for the C−C bond formation. On the other hand, organosilanes and organostannanes have been frequently used as key reagents for many synthetically important transformations. In particular, Lewis acid promoted carbon−carbon bond formation reactions of organosilanes and organostannanes have found considerable interest in organic synthesis in recent years.[7−12] Hydrosilanes and hydrostannanes are also commonly used as convenient hydride reagents in the reduction of various substrates.[10−13] Although these metal hydrides are also regarded as potential electron donors as well as hydride or hydrogen donors,[14] little is known about the actual roles in the electron transfer reactions. No mechanistic comparison has so far been made between the thermal and photochemical reactions of organosilanes and organostannanes with the same substrates. Of many hydride acceptors, nicotinamide adenine dinucleotide (NAD^+) and its analogues are particularly important in regard to the vital role in biological redox processes. The regioselective reduction of NAD^+ analogues has attracted considerable interest in relation with the biological hydride reduction occurring selectively at the C-4 position.[15,16]

We report herein that the photochemical reduction of the 10-methylacridinium ion ($AcrH^+$) by allylic silanes and stannanes

* To whom correspondence should be addressed. E-mail: fukuzumi@ap.chem.eng.osaka-u.ac.jp.
† Osaka University.
‡ Present address: Faculty of Science, Himeji Insutitute of Technology, Kamigori, Hyogo 678-1297, Japan.
§ Tohoku University.

10.1021/jp003518y CCC: $20.00
Published on Web 02/10/2001

occurs efficiently and regioselectively to afford the allylated dihydroacridines in which the allylic group is introduced at the α position but that the thermal reduction by allylic stannanes occurs with the reversed regioselectivities to give the γ adducts.[17] *Reversed* regioselectivities in the photoreduction of NAD^+ analogues (1-methylquinolinium ions) by hydrostannanes and hydrosilanes are also reported as compared to those in the thermal reduction by hydrostannanes and hydrosilanes. We could observe the transient absorption spectra in the visible region successfully to clarify the detailed mechanism of the regioselective photochemical reduction of $AcrH^+$ by organosilanes. Thus, this study provides excellent opportunities to compare directly the regioselectivities in both the thermal and photochemical reduction of NAD^+ analogues by the organometallic compounds and to gain comprehensive and confirmative understanding for their mechanistic difference which leads to the regioreversed addition.

Experimental Section

Materials. 10-Methylacridinium iodide was prepared by the reaction of acridine with methyl iodide in acetone and was converted to the perchlorate salt ($AcrH^+ClO_4^-$) by the addition of magnesium perchlorate to the iodide salt. $AcrH^+ClO_4^-$ was purified by recrystallization from methanol.[18,19] Likewise, 1-methylquinolinium perchlorate ($QuH^+ClO_4^-$), 1,2-dimethylquinolinium perchlorate (2-$MeQuH^+ClO_4^-$), and 1,4-dimethylquinolinium perchlorate (4-$MeQuH^+ClO_4^-$) were prepared by the reaction of the corresponding quinoline derivatives with methyl iodide in acetone, followed by the metathesis with magnesium perchlorate.[18,19] Allyltrimethylsilane and benzyltrimethylsilane were obtained commercially. The other organosilane and organostannane compounds were prepared according to the literature method.[20] Hydrosilanes employed in this study are commercially available. An inorganic oxidant used in this study, tris(1,10-phenanthroline)iron(III) hexafluorophosphate, $[Fe(phen)_3](PF_6)_3$, was prepared according to the literature.[21] Organic oxidants 9,10-dicyanoanthracene, naphthalene, pyrene, and 2,3-dichloro-5,6-dicyano-*p*-benzoquinone were obtained commercially and purified by the standard method.[22] Tetrabutylammonium fluoride was also obtained commercially. Acetonitrile and dichloromethane used as solvents were purified and dried by the standard procedure.[22] [$^2H_3$]acetonitrile (99.5%, Aldrich) was used without further purification.

Reaction Procedure. Typically, an [$^2H_3$]acetonitrile (CD_3CN) solution (0.8 cm^3) containing $AcrH^+$ (1.0×10^{-2} M) in an NMR tube sealed with a rubber septum was deaerated by bubbling with argon gas through a stainless steel needle for 5 min. After an organosilane or organostannane compound (2−5 μL) was added to the solution by means of a microsyringe and mixed, the solution was irradiated with a high-pressure mercury lamp through an acetophenone−methanol filter transmitting $\lambda > 300$ nm at room temperature or in refrigerant methanol thermostated at 233 K by Cryocool CC-100. After the reaction was completed, when the solution became colorless, the reaction solution was analyzed by ^1H NMR spectroscopy. When dichloromethane was used as a solvent, the solvent was pumped off after the reaction. The residue was dried in vacuo and dissolved in CD_3CN, which was then analyzed by ^1H NMR.

Thermal reduction of $AcrH^+$ by an organostannane compound was started by adding an organostannane compound (2×10^{-2} M) to an [$^2H_3$]acetonitrile (CD_3CN) solution (0.8 cm^3) containing $AcrH^+$ (1×10^{-2} M) in an NMR tube. After the reactions were completed, the products were also analyzed by ^1H NMR.

The reaction of QuH^+ (1.0×10^{-1} M) and Ph_3SiH (3.0×10^{-1} M) was started by adding a CD_3CN solution (0.3 cm^3) of tetrabutylammonium fluoride (2.0 M) to a deaerated CD_3CN solution (0.8 cm^3) in an NMR tube sealed with a rubber septum by means of a microsyringe. After the reaction was completed in 1 h, the reaction solution was analyzed by ^1H NMR spectroscopy. In the case of the photoreduction of the 1-methylquinolinium ion (QuH^+), a deaerated CD_3CN solution (0.6 cm^3) of QuH^+ (1.0×10^{-2} M) and tris(trimethylsilyl)silane (1.5×10^{-2} M) in an NMR tube was irradiated with a high-pressure mercury lamp for 50 min.

The ^1H NMR measurements were performed using Japan Electron Optics JNM-PS-100 (100 MHz) and JNM-GSX-400 (400 MHz) NMR spectrometers. ^1H NMR (CD_3CN): AcrH($CH_2CH{=}CH_2$) δ 2.26 (t, 2H, $J = 7.3$ Hz), 3.36 (s, 3H), 3.96 (t, 1H, $J = 7.3$ Hz), 4.76 (dd, 1H, $J = 2.0$, 17 Hz), 4.87 (dd, 1H, $J = 2.0$, 10.3 Hz), 5.68 (m, 1H), 6.9−7.2 (m, 8H); AcrH($CH_2CH{=}CMe_2$) δ 0.89 (s, 3H), 0.93 (s, 3H), 2.21 (t, 2H, $J = 7.3$ Hz), 3.40 (s, 3H), 3.89 (t, 1H, $J = 7.3$ Hz), 5.10 (t, 1H, $J = 7.3$ Hz), 6.95−7.29 (m, 8H); AcrH($CMe_2CH{=}CH_2$) δ 0.84 (s, 6H), 3.30 (s, 3H), 3.73 (s, 1H), 4.45 (dd, 1H, $J = 2.0$, 17.6 Hz), 4.74 (dd, 1H, $J = 2.0$, 10.7 Hz), 5.69 (dd, 1H, $J = 10.7$, 17.6 Hz), 6.9−7.2 (m, 8H); AcrH($CH(Ph)CH{=}CH_2$) δ 3.24 (s, 3H), 3.39 (t, 1H, $J = 8.7$ Hz), 4.19 (d, 1H, $J = 8.3$ Hz), 4.65 (dd, 1H, $J = 2.0$, 17.8 Hz), 4.84 (dd, 1H, $J = 2.0$, 10.3 Hz), 6.0−6.2 (m, 1H), 6.6−7.4 (m, 13H); AcrH($CH_2CH{=}CHPh$) δ 2.2 (m, 2H), 3.37 (s, 3H), 4.10 (t, 1H, $J = 6.8$ Hz), 6.0−7.4 (m, 15H); AcrH(*cyclo*-C_6H_{11}) δ 0.8−2.0 (m, 11H), 3.34 (s, 3H), 3.61 (d, 1H, $J = 8.7$ Hz), 6.6−7.4 (m, 8H); AcrH(CH_2Ph) δ 2.80 (d, 2H, $J = 7.3$ Hz), 3.32 (s, 3H), 4.19 (t, 1H, $J = 7.3$ Hz), 6.7−7.3 (m, 13H); 1,2-QuH_2 δ 2.72 (s, 3H), 3.98 (d, 2H, $J = 3.5$ Hz), 5.73 (m, 1H), 6.32 (d, 1H, $J = 4.2$ Hz), 6.5−7.1 (m, 4H); 1,4-QuH_2 δ 3.01 (s, 3H), 3.52 (d, 2H, $J = 3.3$ Hz), 4.51 (m, 1H), 5.73 (d, 1H, $J = 9.6$ Hz), 6.7−7.2 (m, 4H); 2-Me-1,2-QuH_2 δ 1.05 (d, 3H, $J = 5.3$ Hz), 2.81 (s, 3H), 4.08 (m, 1H), 5.72 (dd, 1H, $J = 9.1$, 4.2 Hz), 6.31 (d, 1H, $J = 9.1$ Hz), 6.5−7.1 (m, 4H); 2-Me-1,4-QuH_2 δ 2.05 (s, 3H), 3.20 (s, 3H), 3.48 (d, 2H, $J = 3.3$ Hz), 5.95 (m, 1H), 6.8−7.4 (m, 4H); 4-Me-1.2-QuH_2 δ 1.95 (s, 3H), 2.70 (s, 3H), 3.86 (d, 2H, $J = 4.1$ Hz), 5.60 (t, 1H, $J = 4.1$ Hz), 6.5−7.1 (m, 4H); 4-Me-1,4-QuH_2 δ 1.15 (d, 3H, $J = 6.5$ Hz), 3.02 (s, 3H), 3.40 (m, 1H), 6.6−7.4 (m, 6H).

Kinetic Measurements. Kinetic measurements were performed under deaerated conditions using a Shimadzu UV-160A, UV-2200, or a Hewlett-Packard diode array spectrophotometer (HP8452), which was thermostated at 298 K. Rates of the electron-transfer reactions from organostannanes to the ferricenium ion in MeCN were followed by the decrease in absorbance because of ferricenium ion in the long-wavelength region (600−700 nm).[23] A typical procedure for the kinetic measurements of the thermal reactions of $AcrH^+$ and X-QuH^+ with organostannanes is the following. An acetonitrile (0.40 cm^3) solution of 2.7×10^{-3} M $AcrH^+$ or X-QuH^+ contained in a 1 mm quartz cuvette was placed in a cell holder of the spectrophotometer, which was thermostated at 298 K. Allylstannane was added ($2-6 \times 10^{-2}$ M) by means of a microsyringe with shaking. Rates of the reduction of $AcrH^+$ and X-QuH^+ were followed by the disappearance of the absorbance ($\lambda = 415$ and 315 nm) due to $AcrH^+$ and X-QuH^+, respectively. The pseudo-first-order plot for each reaction was linear for three or more half-lives with the correlation coefficient $\rho > 0.999$.

Quantum Yield Determinations. A standard actinometer (potassium ferrioxalate)[24] was used for the quantum yield determination of the photoreduction of $AcrH^+$ and X-QuH^+ by organometallic compounds. A square quartz cuvette (10 mm i.d.) which contained an acetonitrile solution (3.0 cm^3) of $AcrH^+$

and X-QuH$^+$ ($3.1-6.0 \times 10^{-4}$ M) and an organometallic compound ($5 \times 10^{-4}-4 \times 10^{-3}$ M) was irradiated with monochromatized light of $\lambda = 358$ and 320 nm from a Hitachi 650-10S fluorescence spectrophotometer, respectively. Under the conditions of the actinometry experiments, both the actinometer and AcrH$^+$ or X-QuH$^+$ absorbed essentially all of the incident light. The light intensity of monochromatized light of $\lambda = 358$ and 320 nm was determined as 1.1×10^{-8} and 3.8×10^{-8} einstein s^{-1} with the slit width of 20 nm, respectively. The photochemical reaction was monitored by using a Shimadzu UV-160A or UV-2200 spectrophotometer. The quantum yields were determined from the decrease in the absorbance because of AcrH$^+$ ($\lambda = 396$ nm, $\epsilon = 3.5 \times 10^3$ M^{-1} cm^{-1}) and QuH$^+$ ($\lambda = 338$ nm, $\epsilon = 1.8 \times 10^3$ M^{-1} cm^{-1}). When the contribution of thermal reactions cannot be neglected, the quantum yields were determined by subtracting the rate of thermal reactions in the dark from that of the photochemical reaction.

Fluorescence Quenching. Quenching experiments of the fluorescence of the 10-methylacridinium ion, 9,10-dicyanoanthracene, naphthalene, and pyrene by organosilanes and organostannanes were performed using a Hitachi 650-10S fluorescence spectrophotometer. The excitation wavelengths were 360, 315, 390, 300, and 365 nm for AcrH$^+$, QuH$^+$, 9,10-dicyanoanthracene, naphthalene, and pyrene in MeCN, respectively. The monitoring wavelengths were those corresponding to the maxima of the emission bands at $\lambda = 488$, 398, 460, 335, and 420 nm, respectively. The solutions were deoxygenated by argon purging for 10 min prior to the measurements. Relative emission intensities were measured for MeCN solution containing AcrH$^+$ or QuH$^+$ (5.0×10^{-5} M) with organometals at various concentrations ($1.5-6.2 \times 10^{-2}$ M). There was no change in the shape but there was a change in the intensity of the fluorescence spectrum by the addition of an organometal. The Stern−Volmer relationship (eq 1) was obtained for the ratio of the emission intensities in the absence and presence of organometals (I_0/I) and the concentrations of organometals [D]. The fluorescence lifetime τ of AcrH$^+$ was determined as 37 ns in MeCN by single-photon counting using a Horiba NAES-1100 time-resolved spectrofluorophotometer. The observed quenching rate constants k_q ($= K_{SV}\tau^{-1}$) were obtained from the Stern−Volmer constants K_{SV} and the emission lifetimes τ. When organometals such as allyltributylstannane which reacts thermally with AcrH$^+$ are employed as quenchers, the Stern−Volmer constant (K_{SV}) was determined from the ratio of the lifetime in the absence and presence of organometals (τ_0/τ) by use of a single-photon counting using a Horiba NAES-1100 time-resolved spectrofluorophotometer (eq 2).

$$I_0/I = 1 + K_{SV}[D] \quad (1)$$

$$\tau_0/\tau = 1 + K_{SV}[D] \quad (2)$$

Laser-Flash Photolysis. The measurements of transient absorption spectra in the photochemical reactions of AcrH$^+$ with $PhCH_2SiMe_3$ or $CH_2{=}CHCH_2SiMe_3$ in MeCN were performed according to the following procedures. The MeCN solution was deoxygenated by argon purging for 10 min prior to the measurement. The deaerated MeCN solution containing AcrH$^+$ (1.7×10^{-3} M) and organosilanes (2.8×10^{-2} M) was excited by a Nd:YAG laser (Quanta-Ray, GCR-130, 6 ns fwhm) at 355 nm with the power of 30 mJ. A pulsed xenon flash lamp (Tokyo Instruments, XF80-60, 15 J, 60 ms fwhm) was used for the probe beam, which was detected with a Si PIN photodiode (Hamamatsu, S1722-02) after passing through the photochemical quartz vessel (10×5 mm) and a monochromator. The output from the Si PIN photodiode was recorded with a digitizing oscilloscope (HP 54510B, 300 MHz). The transient spectra were recorded using fresh solutions in each laser excitation. All experiments were performed at 298 K.

ESR Measurements. ESR spectra of the photolyzed AcrH$^+$ClO$_4^-$ and $PhCH_2SiMe_3$ (or ferrocene) in frozen MeCN were taken on a JEOL JES-RE1XE and were recorded under nonsaturating microwave power conditions. The magnitude of the modulation was chosen to optimize the resolution and the signal-to-noise ratio (S/N) of the observed spectra. The g values were calibrated using an Mn^{2+} marker.

Theoretical Calculations. Semiempirical calculations were performed using the MOPAC program (version 6) which is incorporated in the MOLMOLIS program (version 2.8) by Daikin Industries, Co., Ltd. The PM3 Hamiltonian was used for the semiempirical MO calculations.[25] Final geometries and energetics were optimized by minimizing the total molecular energy with respect to all structural variables. The heats of formation (ΔH_f) were calculated with the restricted Hartree−Fock (RHF) formalism using a key word "PRECISE". The ab initio calculations were performed at the Becke3LYP/6-31+G* or MP2/6-31++G* level[26,27] with Gaussian 98.[28]

Results and Discussion

Photoaddition of Organosilanes and Organostannanes with the 10-Methylacridinium Ion. Irradiation of the absorption band of 10-methylacridinium perchlorate (AcrH$^+$ClO$_4^-$) in a deaerated acetonitrile solution containing allylsilane for 3.5 h gave an adduct [AcrH($CH_2CH{=}CH_2$)] as shown in eq 3. Such

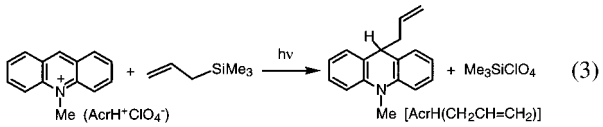

(3)

photoaddition reactions with AcrH$^+$ also occur efficiently using other organosilanes and organostannanes. The products are well identified by the ^{1}H NMR spectra (see the Experimental Section). The product yields under various reaction conditions are summarized in Table 1. When an unsymmetrical allylic silane, e.g, prenyltrimethylsilane, is employed, the allylic group is introduced at the α position to yield AcrH($CH_2CH{=}CMe_2$) exclusively and no γ adduct [AcrH($CMe_2CH{=}CH_2$)] has been formed (eq 4). In the case of prenyltributylstannane, however,

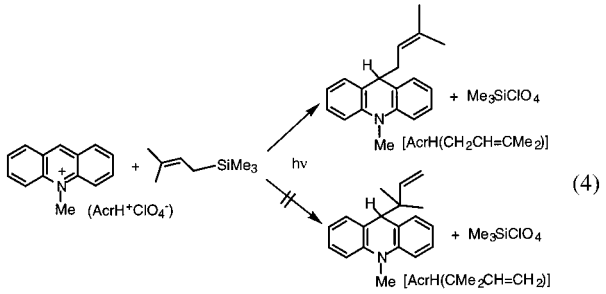

(4)

γ adduct (20%) is formed as well as α adduct which is the major product. Although the addition reaction of prenyltributylstannane with AcrH$^+$ also occurs thermally to yield the γ adduct exclusively as described later, the photoaddition reaction was carried out under the experimental conditions such that the contribution of the thermal reaction can be neglected. In fact, essentially the same selectivity ratio of the α to γ adduct was

TABLE 1: Photoreduction of $AcrH^+$ (1.0×10^{-2} M) by Organosilanes and Organostannanes (1.5×10^{-2} M) in Deaerated MeCN

allylmetal	condition	time (h)	product (yield, %)
$CH_2{=}CHCH_2SiMe_3$	*a*	3.5	$AcrH(CH_2CH{=}CH_2)$ (60)
$Me_2C{=}CHCH_2SiMe_3$	*a*	3.5	$AcrH(CH_2CH{=}CMe_2)$ (60)
$PhCH_2SiMe_3$	*a*	1.5	$AcrH(CH_2Ph)$ (100)
$CH_2{=}CHCH_2SnPh_3$	*a*	1.5	$AcrH(CH_2CH{=}CH_2)$ (85)
$PhCH_2SnPh_3$	*a*	1.0	$AcrH(CH_2Ph)$ (100)
$CH_2{=}CHCH_2SnBu_3$	*a*	0.5	$AcrH(CH_2CH{=}CH_2)$ (100)
$Me_2C{=}CHCH_2SnBu_3$	*a*	0.5	$AcrH(CH_2CH{=}CMe_2)$ (80) $AcrH(CMe_2CH{=}CH_2)$ (20)
$Me_2C{=}CHCH_2Sn(cyclo\text{-}C_6H_{11})_3$	*a*	1.0	$AcrH(CH_2CH{=}CMe_2)$ (67) $AcrH(CMe_2CH{=}CH_2)$ (16) $AcrH(cyclo\text{-}C_6H_{11})$ (17)
$PhCH{=}CHCH_2SnBu_3$	*a*	0.5	$AcrH(CH_2CH{=}CHPh)$ (57) $AcrH(C(H)PhCH{=}CH_2)$ (43)
$Me_2C{=}CHCH_2SnBu_3$	*b*	1.0	$AcrH(CH_2CH{=}CMe_2)$ (81) $AcrH(CMe_2CH{=}CH_2)$ (19)
$Me_2C{=}CHCH_2SnBu_3$	*c*	1.0	$AcrH(CH_2CH{=}CMe_2)$ (100)
$Me_2C{=}CHCH_2Sn(cyclo\text{-}C_6H_{11})_3$	*c*	1.0	$AcrH(CH_2CH{=}CMe_2)$ (71) $AcrH(CMe_2CH{=}CH_2)$ (11) $AcrH(cyclo\text{-}C_6H_{11})$ (18)

[a] In MeCN at 298 K. [b] In MeCN at 233 K. [c] $[AcrH^+] = 6.1 \times 10^{-3}$ M, [organometal] $= 1 \times 10^{-2}$ M in CH_2Cl_2 at 298 K.

TABLE 2: Addition Reaction of Allylic Stannanes with $AcrH^+$ in MeCN in the Dark

allylic stannane (concentration; M)	$[AcrH^+]$ (M)	time (h)	product (yield, %)
$CH_2{=}CHCH_2SnBu_3$[a] (8.0×10^{-2})	6×10^{-2}	1	$AcrH(CH_2CH{=}CH_2)$ (100)
$Me_2C{=}CHCH_2SnBu_3$[a] (2.0×10^{-2})	1×10^{-2}	10	$AcrH(CMe_2CH{=}CH_2)$ (100)
$Me_2C{=}CHCH_2Sn(cyc\text{-}C_6H_{11})_3$[a] ($3.8 \times 10^{-2}$)	1×10^{-2}	10	$AcrH(CMe_2CH{=}CH_2)$ (100)
$PhCH{=}CHCH_2SnBu_3$[a] (1.5×10^{-2})	1×10^{-2}	10	$AcrH(C(H)PhCH{=}CH_2)$ (100)
$Me_2C{=}CHCH_2SnBu_3$[b] (2.9×10^{-2})	4×10^{-3}	10	$AcrH(CMe_2CH{=}CH_2)$ (100)
$Me_2C{=}CHCH_2Sn(cyc\text{-}C_6H_{11})_3$[b] ($3.7 \times 10^{-2}$)	4×10^{-3}	10	$AcrH(CMe_2CH{=}CH_2)$ (100)

[a] In MeCN. [b] In CH_2Cl_2.

TABLE 3: Observed Rate Constants (k_{obs}) of the Thermal Reduction of $AcrH^+$ (2.7×10^{-3} M) by Allylic Stannanes in MeCN at 298 K

allylic stannane	k_{obs} ($M^{-1}\,s^{-1}$)
$CH_2{=}CHCH_2SnBu_3$	6.4×10^{-2}
$Me_2C{=}CHCH_2SnBu_3$	1.4×10^{-2}
$PhCH{=}CHCH_2SnBu_3$	5.2×10^{-3}

obtained at a much lower reaction temperature (233 K) when the contribution of the thermal reaction, if any, should be completely neglected as compared to the reaction at 298 K (Table 1). The yield of γ adduct is increased to 43% which is comparable with that of the α adduct (57%) when tributyl-*trans*-cinnamylstannane is employed (Table 1).

When the butyl group of prenyltributylstannane is replaced by the more-electron-donating cyclohexyl group, the adduct derived from the cleavage of the Sn−cyclohexyl group is also obtained together with the α and γ adducts of the allylic group (Table 1). The ratio of the α to γ adduct increases when CH_2Cl_2 instead of MeCN is used as a solvent (Table 1).

The photoalkylation also occurs selectively in the case of organosilanes containing an electron-donating alkyl group, e.g., benzyltrimethylsilane, to yield the benzyl adduct (Table 1). We have previously reported that photoalkylation of $AcrH^+$ by tetraalkyltin compounds (R_4Sn, R = Et, Bu, and Pr^i) to yield AcrHR.[29]

Thermal Reduction of the 10-Methylacridinium Ion by Allylic Stannanes. It is found that the 10-methylacridinium ion ($AcrH^+$) is readily reduced by allyltributyltin to yield selectively 9-allyl-10-methyl-9,10-dihydroacridine [$AcrH(CH_2CH{=}CH_2)$] in MeCN as shown in Table 2. In contrast to the photochemical reaction (Table 1), the thermal reaction of $AcrH^+$ with prenyltributylstannane yields only the γ adduct (eq 5). Likewise the

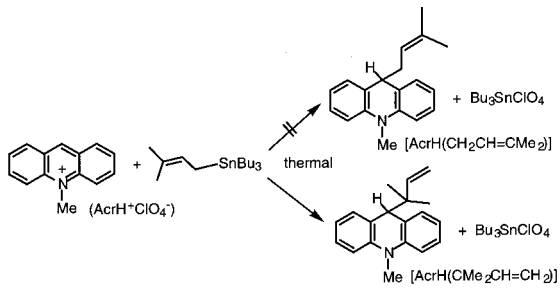

(5)

thermal reduction of $AcrH^+$ by tributyl-*trans*-cinnamylstannane also yield the γ adduct exclusively (Table 2).

Rates of the reduction of $AcrH^+$ by allylic stannanes were followed by the disappearance of the absorbance ($\lambda = 415$ nm) because of $AcrH^+$ (see the Experimental Section). The rates obeyed ordinary second-order kinetics, showing the first-order dependence on the concentration of each reactant. The observed second-order rate constants (k_{obs}) are listed in Table 3. The k_{obs} value decreases with the γ substitution by the bulky groups (Me_2 and Ph), demonstrating a significant steric effect of the substituent at the carbon where the C−C bond is formed with $AcrH^+$.

Thermal Hydride Reduction of NAD$^+$ Analogues. Upon mixing QuH^+ (8.0×10^{-5} mol) with Bu_3SnH (1.9×10^{-4} mol) in acetonitrile (0.80 cm^3) at 298 K, QuH^+ was readily reduced to yield initially 1-methyl-1,2-dihydroquinoline (1,2-QuH_2; 80% in 30 min), which was gradually isomerized to the corresponding 1,4 isomer (1,4-QuH_2; 70% in 70 min) as shown in eq 6. The

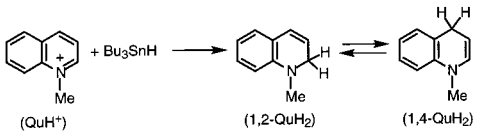

(6)

1,2 and 1,4 isomers can also be differentiated by their absorption spectra (λ_{max} = 350 and 250 nm, respectively). Figure 1 shows the electronic spectra observed in the reduction of QuH^+ by Bu_3SnH in MeCN. Under the experimental conditions of a low concentration of QuH^+ (2.0×10^{-3} M), the absorbance due to the initial product, the 1,2 isomer (λ_{max} = 350 nm), increases, accompanied by the decrease in absorbance because of QuH^+ (λ_{max} = 315 nm) with a clean isosbestic point. The reduction of the 1,4-dimethylquinolinium ion (4-$MeQuH^+$) by Bu_3SnH also occurs efficiently to yield exclusively the corresponding 1,2 isomer (4-Me-1,2-QuH_2) which does not isomerize to the 1,4 isomer. These products were well identified from their ^{1}H NMR spectra (see the Experimental Section). The isomerization from 1,2-QuH_2 to 1,4-QuH_2 has been reported to occur by the reaction of the 1,2 isomer with QuH^+ in the reduction of quinolinium salts with $NaBH_4$.[30] When QuH^+ is replaced by the 1,2-dimethylquinolinium ion (2-$MeQuH^+$) in which the C-2 position is blocked by the methyl group, no reaction with Bu_3SnH has occurred at 298 K.

Various hydrosilanes are known to be capable of reducing carbonyl compounds in the presence of fluoride ions, when pentacoordinate hydrosilicates $[R_3SiHF]^-$ are formed as reactive intermediates.[31] In the present system as well, the addition of fluoride ions ($Bu_4N^+F^-$) to the Ph_3SiH-QuH^+ system results in the efficient reduction of QuH^+ to yield 1,2-QuH_2 selectively (eq 7), although hydrosilanes are inactive toward QuH^+ without F^- in MeCN. The product yields of the reduction of QuH^+,

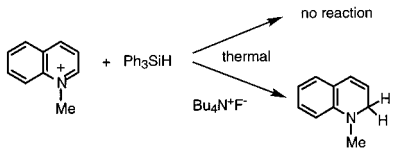

(7)

2-$MeQuH^+$, and 4-$MeQuH^+$ by various hydrosilanes in the presence of fluoride ion are listed in Table 4.

The isomerization from the initial product, 1,2-QuH_2, to 1,4-QuH_2 is also observed in the reduction of QuH^+ by Ph_3SiH in the presence of fluoride ions in MeCN (Table 4) as the case of the reduction by Bu_3SnH (eq 6). The reduction of 4-$MeQuH^+$ by hydrosilanes also occurs efficiently in the presence of fluoride ion in MeCN to yield exclusively 4-Me-1,2-QuH_2 which does not isomerize to the corresponding 1,4 isomer (Table 4). In contrast with the case of Bu_3SnH, the reduction of 2-$MeQuH^+$ by hydrosilanes also occurs efficiently in the presence of fluoride ion to yield 2-Me-1,2-QuH_2 selectively (Table 4). Thus, hydrosilanes in the presence of fluoride ions act as strong hydride reagents as compared with the hydrostannane Bu_3SnH.

The ΔH_f (heat of formation) values of 1,2-QuH_2 and 1,4-QuH_2 are calculated as 37.3 and 34.1 kcal mol^{-1} by using the PM3 semiempirical MO method with the geometrical parameters optimized (see the Experimental Section). Thus, the initial nucleophilic attack of Bu_3SnH and hydrosilanes in the presence of the fluoride ion occurs preferentially at the C-2 position in the case of QuH^+ to yield the 1,2 isomer, which then isomerizes to the thermodynamically stable form, the 1,4 isomer.

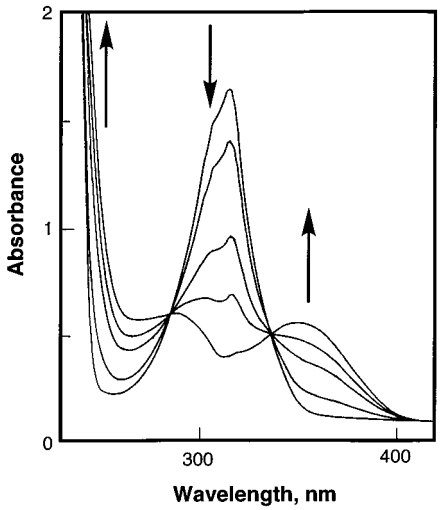

Figure 1. Electronic absorption spectra observed in the reduction of QuH^+ (2.0×10^{-3} M) by Bu_3SnH (2.0×10^{-2} M) in MeCN at 298 K. Time interval: 0, 10, 30, 45, and 60 min.

TABLE 4: Regioselective Reduction of QuH$^+$ Derivatives by Hydrosilanes in the Presence of $Bu_4N^+F^-$ (0.2 M) and by Bu_3SnH in MeCN at 298 K

metal hydride (M)	QuH^+ derivative (0.1M)	time (h)	product (yield, %)
Ph_3SiH (0.2)	QuH^+	1	1,2-QuH_2 (100)
		3	1,2-QuH_2 (94)
			1,4-QuH_2 (6)
		24	1,2-QuH_2 (58)
			1,4-QuH_2 (42)
		100	1,2-QuH_2 (39)
			1,4-QuH_2 (61)
Ph_2SiH_2 (0.3)	QuH^+	1	1,2-QuH_2 (55)
			1,4-QuH_2 (45)
$PhMe_2SiH$ (0.3)	QuH^+	1	1,2-QuH_2 (100)
$(MeO)_3SiH$ (0.3)	QuH^+	2	1,2-QuH_2 (100)
$(TMS)_3SiH$ (0.3)	QuH^+	2	1,2-QuH_2 (87)
			1,4-QuH_2 (13)
Bu_3SnH (0.24)[a]	QuH^+	1	1,2-QuH_2 (40)
			1,4-QuH_2 (60)
Ph_3SiH (0.2)	2-$MeQuH^+$	3	2-Me-1,2-QuH_2 (100)
Ph_2SiH_2 (0.3)	2-$MeQuH^+$	1	2-Me-1,2-QuH_2 (100)
$PhMe_2SiH$ (0.3)	2-$MeQuH^+$	1	2-Me-1,2-QuH_2 (100)
$(MeO)_3SiH$ (0.3)	2-$MeQuH^+$	2	2-Me-1,2-QuH_2 (100)
$(TMS)_3SiH$ (0.3)	2-$MeQuH^+$	2	2-Me-1,2-QuH_2 (100)
Bu_3SnH (0.24)[a]	2-$MeQuH^+$	1	no reaction
Ph_3SiH (0.2)	4-$MeQuH^+$	3	4-Me-1,2-QuH_2 (100)
Ph_2SiH_2 (0.3)	4-$MeQuH^+$	1	4-Me-1,2-QuH_2 (100)
$PhMe_2SiH$ (0.3)	4-$MeQuH^+$	1	4-Me-1,2-QuH_2 (100)
$(MeO)_3SiH$ (0.3)	4-$MeQuH^+$	2	4-Me-1,2-QuH_2 (100)
$(TMS)_3SiH$ (0.3)	4-$MeQuH^+$	2	4-Me-1,2-QuH_2 (100)
Bu_3SnH (0.24)[a]	4-$MeQuH^+$	1	4-Me-1,2-QuH_2 (100)

[a] In the absence of $Bu_4N^+F^-$.

Photochemical Reduction of Quinolinium Ions by Bu_3SnH and $(TMS)_3SiH$. As described above, no thermal reduction of 2-$MeQuH^+$ by Bu_3SnH occurs because of the steric effect of the methyl group at the C-2 position. Irradiation of the absorption band of 2-$MeQuH^+$ (λ_{max} = 315 nm) in deaerated MeCN containing Bu_3SnH with monochromatized light of λ = 320 nm, however, results in the efficient reduction of 2-$MeQuH^+$ to yield the corresponding 1,4 isomer (2-Me-1,4-QuH_2) exclu-

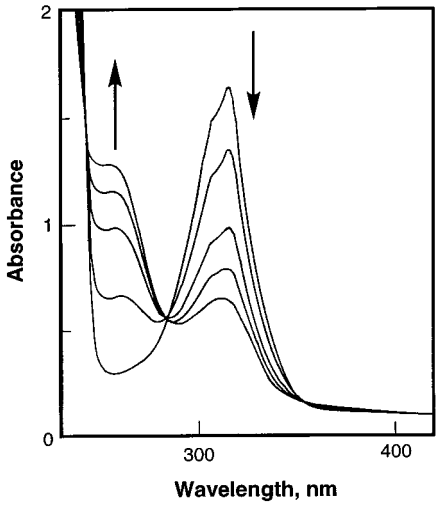

Figure 2. Electronic absorption spectra observed in the photoreduction of QuH^+ (2.0×10^{-3} M) by $(TMS)_3SiH$ (2.0×10^{-2} M) in MeCN at 298 K. Time interval: 0, 10, 30, 40, and 50 min.

sively (eq 8). In contrast to the thermal reduction of QuH^+ by

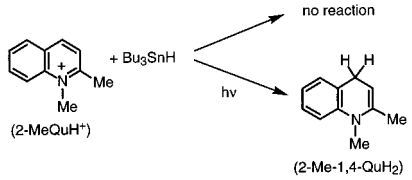

(8)

Bu_3SnH, no 1,2 isomer has been formed during the photochemical reaction. When Bu_3SnH is replaced by $(TMS)_3SiH$ (TMS = trimethylsilyl), no thermal reduction of X-QuH^+ (X = H, 2-Me, and 4-Me) by $(TMS)_3SiH$ has occurred at 298 K. As is the case of the photochemical reaction of 2-$MeQuH^+$ with Bu_3SnH, irradiation of the absorption band of X-QuH^+ in deaerated MeCN containing $(TMS)_3SiH$ and H_2O (5.0 M) results in the efficient reduction of X-QuH^+ to yield the corresponding 1,4 isomer (X-1,4-QuH_2) exclusively (H_2O was added to trap the silyl cation). Figure 2 shows the electronic spectra observed in the photoreduction of QuH^+ by $(TMS)_3SiH$ in deaerated MeCN. In contrast to the thermal reduction of QuH^+ by Bu_3SnH (Figure 1), the absorbance due to the initial product, the 1,4 isomer (λ_{max} = 250 nm), increases, accompanied by the decrease in absorbance because of QuH^+ (λ_{max} = 315 nm) with a clean isosbestic point. The photoreduction of 2-$MeQuH^+$ and 4-$MeQuH^+$ by $(TMS)_3SiH$ also occurs efficiently to yield the corresponding 1,4 isomers. In the case of the photoreduction of the 10-methylacridinium ion ($AcrH^+$) by $(TMS)_3SiH$, 10-methyl-9,-10-dihydroacridine ($AcrH_2$) is obtained exclusively. The product yields of the photoreduction of these NAD^+ analogues by $(TMS)_3SiH$ are listed in Table 5.

Photoinduced Electron Transfer. Irradiation of the absorption bands of $AcrH^+$ and QuH^+ in MeCN causes fluorescence at 488 and 398 nm, respectively. The fluorescence of $AcrH^+$ is known to be quenched by electron transfer from various organic electron donors to the singlet excited state ($AcrH^{+}$*).[32] The fluorescences of $AcrH^+$, QuH^+, 2-$MeQuH^+$, and 4-$MeQuH^+$ are also quenched efficiently by electron donors including organosilanes and organostannanes employed in this study. The rate constants (k_{obs}) of the fluorescence quenching are determined from the slopes of the Stern−Volmer plots and lifetimes of the singlet excited state [$AcrH^{+}$* (τ = 37 ns), QuH^{+}* (20 ns), 2-$MeQuH^{+}$* (15 ns), and 4-$MeQuH^{+}$* (19 ns)], which were determined by the single-photon counting measurements (see the Experimental Section). The free-energy change of photoinduced electron transfer from organosilanes and organostannanes to these singlet excited states (ΔG^0_{et} in eV) is given by eq 9:

$$\Delta G^0_{et} = e(E^0_{ox} - E^0_{red}) \quad (9)$$

where e is the elementary charge, E^0_{ox} is the one-electron oxidation potentials of organosilanes[6a,33] and organostannanes,[17] and E^0_{red} is the one-electron reduction potentials of the singlet excited states, $AcrH^{+}$* and X-QuH^{+}* (X = H, 2-Me, and 4-Me).[34] The ΔG^0_{et} values are largely negative as listed in Table 6, indicating that the fluorescence quenching occurs efficiently via photoinduced electron transfer from organosilanes and organostannanes to $AcrH^{+}$* and X-QuH^{+}*. The rate constants (k_{obs}) of the fluorescence quenching via photoinduced electron transfer are listed in Table 6, where the k_{obs} values are in the range of $1.0-1.7 \times 10^{10}$ M^{-1} s^{-1}, being close to the diffusion limit in MeCN at 298 K.[35] The k_{obs} values for photoinduced electron transfer and thermal electron transfer reactions of organosilanes and organostannanes are also included in Table 6. A plot of log k_{obs} vs ΔG^0_{et} is shown in Figure 3, which demonstrates a typical dependence of the rate constant for outer-sphere electron-transfer reactions on the free-energy change of electron transfer (ΔG^0_{et}); the log k_{obs} value increases with a decrease in ΔG^0_{et} to reach a diffusion-limited value ($k_{obs} = 2.0 \times 10^{10}$ M^{-1} s^{-1}).[35]

A general scheme for photoinduced electron transfer from an electron donor (D) to an excited-state acceptor (A*) is given in eq 10:

$$D + A^* \underset{k_{21}}{\overset{k_{12}}{\rightleftharpoons}} (D\ A^*) \xrightarrow{k_{et}} (D^{\bullet+}\ A^{\bullet-}) \xrightarrow{k_{bet}} D + A \quad (10)$$

where k_{12} and k_{21} are diffusion and dissociation rate constants in the encounter complex (D A*) and k_{et} and k_{bet} are the rate constants of forward electron transfer from D to A to produce the radical ion pair ($D^{\bullet+}$ $A^{\bullet-}$) and back electron transfer to the ground state.[6a,35−37] The observed rate constant (k_{obs}) of photoinduced electron transfer is given by eq 11. The dependence

$$k_{obs} = k_{et}k_{12}/(k_{21} + k_{bet}) \quad (11)$$

of k_{et} on ΔG^0_{et} for adiabatic outer-sphere electron transfer has been well established by Marcus as given by eq 12:

$$k_{et} = (kT/h)\exp[-(\lambda/4)(1 + \Delta G^0_{et}/\lambda)^2/kT] \quad (12)$$

where k is the Boltzmann constant, h is the Planck constant, and λ is the reorganization energy of electron transfer.[38−40] From eqs 11 and 12 is derived eq 13:

$$[kT \ln Z(k_{obs}^{-1} - k_{12}^{-1})]^{1/2} = \lambda^{1/2}/2 + \Delta G^0_{et}/(2\lambda^{1/2}) \quad (13)$$

where k_{12} in MeCN is known as 2.0×10^{10} M^{-1} s^{-1} [35] and Z [$= (kT/h)(k_{12}/k_{21})$] is the collision frequency taken as 1×10^{11} M^{-1} s^{-1}.[38] A linear plot of $[kT \ln Z(k_{obs}^{-1} - k_{12}^{-1})]^{1/2}$ [$= (\Delta G^{\ddagger}_{et})^{1/2}$] vs ΔG^0_{et} (eq 13) is shown in Figure 4, where the k_{obs} values with $\Delta G^0_{et} < -0.53$ eV are not included because of the large uncertainty of the $k_{obs}^{-1} - k_{12}^{-1}$ values. From the intercept at $\Delta G^0_{et} = 0$, the λ value is obtained as 0.90 eV. The slope of the linear correlation in Figure 4 (0.48 $eV^{-1/2}$) agrees with the value expected from eq 13, $1/(2\lambda^{1/2}) = 0.48$ $eV^{-1/2}$.

The dependence of k_{obs} on ΔG^0_{et} is calculated based on eq 13 using the λ value (0.90 eV) as shown by the solid line in Figure 3. The k_{obs} values with $\Delta G^0_{et} < -0.53$ eV which were

TABLE 5: Photoreduction of NAD^+ Analogues by $(TMS)_3SiH$ and Bu_3SnH in Deaerated MeCN at 298 K under Irradiation of Light of $\lambda = 320$ nm

metal hydride (0.02 M)	NAD^+ analogue (0.02 M)	irradiation time (min)	product (yield, %)	
$(TMS)_3SiH$	$AcrH^+$	60	$AcrH_2$ (100)	
$(TMS)_3SiH$	QuH^+	50	1,2-QuH_2 (0)	1,4-QuH_2 (62)
$(TMS)_3SiH$	2-MeQuH^+	60	2-Me-1,2-QuH_2 (0)	2-Me-1,4-QuH_2 (60)
$(TMS)_3SiH$	4-MeQuH^+	50	4-Me-1,2-QuH_2 (0)	4-Me-1,4-QuH_2 (50)
Bu_3SnH	2-MeQuH^+	60	2-Me-1,2-QuH_2 (0)	2-Me-1,4-QuH_2 (70)

TABLE 6. Free-Energy Change of Electron Transfer (ΔG^0_{et}), Rate Constants (k_{obs}) of Electron Transfer, and Limiting Quantum Yields (Φ_∞) for the Photochemical Reactions of $AcrH^+$ and QuH^+ Derivatives with Organosilanes and Organostannanes in MeCN at 298 K

acceptor	E^0_{red}[a] (V)	donor[b]	ΔG^0_{et}[c] (eV)	k_{obs}[d] (M^{-1} s^{-1})	k_{obs}[e] (M^{-1} s^{-1})	Φ_∞[e]
$AcrH^+$*	2.32	$Me_2C{=}CHCH_2SnBu_3$	−1.43	1.8×10^{10}	1.4×10^{10}	1.8×10^{-1}
		$CH_2{=}CHCH_2SnBu_3$	−1.26	1.8×10^{10}	1.4×10^{10}	1.5×10^{-1}
		$(TMS)_3SiH$	−1.02	1.2×10^{10}	1.7×10^{10}	8.0×10^{-2}
		$(TMS)_3SiD$	−1.02	1.2×10^{10}	1.7×10^{10}	3.6×10^{-2}
		$PhCH_2SiMe_3$	−0.94	1.2×10^{10}	1.0×10^{10}	1.7×10^{-2}
		$Me_2C{=}CHCH_2SiMe_3$	−0.93	9.0×10^{9}	1.1×10^{10}	7.0×10^{-3}
		$CH_2{=}CHCH_2SiMe_3$	−0.82	1.2×10^{10}	1.0×10^{10}	8.0×10^{-3}
QuH^+*	2.54	$(TMS)_3SiH$	−1.24	1.0×10^{10}	1.3×10^{10}	8.0×10^{-2}
		$(TMS)_3SiD$	−1.24	1.0×10^{10}	1.3×10^{10}	4.2×10^{-2}
2-MeQuH^+*	2.46	$(TMS)_3SiH$	−1.16	1.3×10^{10}	1.7×10^{10}	9.6×10^{-2}
4-MeQuH^+*	2.51	$(TMS)_3SiH$	−1.21	1.0×10^{10}	1.2×10^{10}	7.6×10^{-2}
DCA*	1.91	$Me_2C{=}CHCH_2SnBu_3$	−1.02	1.5×10^{10}		
		$CH_2{=}CHCH_2SnBu_3$	−0.85	1.5×10^{10}		
		$(TMS)_3SiH$	−0.61	6.5×10^{9}		
		$PhCH_2SiMe_3$	−0.53	6.7×10^{9}		
		$Me_2C{=}CHCH_2SiMe_3$	−0.52	9.0×10^{9}		
		$CH_2{=}CHCH_2SiMe_3$	−0.41	3.1×10^{9}		
naphthalene*	1.46	$Me_2C{=}CHCH_2SnBu_3$	−0.57	6.8×10^{9}		
		$CH_2{=}CHCH_2SnBu_3$	−0.40	1.4×10^{9}		
		$Me_2C{=}CHCH_2SiMe_3$	−0.07	1.8×10^{8}		
		$CH_2{=}CHCH_2SiMe_3$	0.04	1.5×10^{7}		
pyrene*	1.23	$Me_2C{=}CHCH_2SnBu_3$	−0.34	5.2×10^{9}		
		$CH_2{=}CHCH_2SnBu_3$	−0.17	1.5×10^{8}		
		$(TMS)_3SiH$	0.07	1.2×10^{7}		
		$PhCH_2SiMe_3$	0.15	9.1×10^{6}		
		$Me_2C{=}CHCH_2SiMe_3$	0.16	2.3×10^{7}		
$Fe(phen)_3^{3+}$	0.98	$(TMS)_3SiH$	0.32	1.0×10^{3}		
$FeCp_2^+$	0.37	$Me_2C{=}CHCH_2SnMe_3$	0.52	5.0		
		$CH_2{=}CHCH_2SnBu_3$	0.69	8.0×10^{-3}		

[a] E^0_{red} vs SCE, taken from refs 6a, 33, and 34. [b] The E^0_{ox} values are taken from refs 6a and 17. [c] Determined from eq 9. [d] Determined from the fluorescence-quenching rate constants for photoinduced electron transfer and electron transfer rate constants for thermal electron transfer reactions. [e] Determined from the dependence of the quantum yield on the donor concentration.

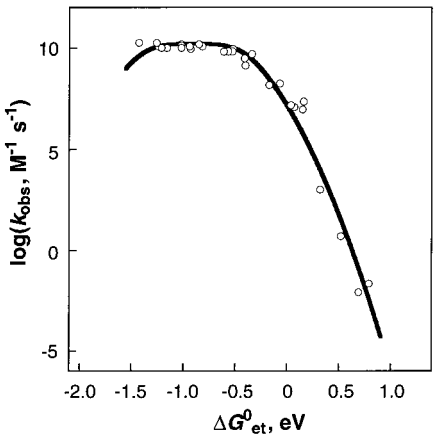

Figure 3. Plot of log k_{obs} vs ΔG^0_{et} for photoinduced and thermal electron transfer reactions of organosilanes and organostannanes in MeCN at 298 K. The data are taken from Table 6. The solid line is drawn on the basis of eq 12 using $\lambda = 0.90$ eV.

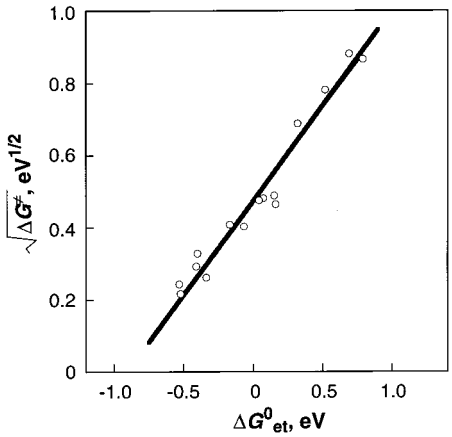

Figure 4. Plot of $(\Delta G^{\ddagger}_{et})^{1/2}$ $(= [kT \ln Z(k_{obs}^{-1} - k_{12}^{-1})]^{1/2})$ vs ΔG^0_{et} (see eq 13). The k_{obs} values with $\Delta G^0_{et} < -0.53$ eV in Table 6 are not included because of the large uncertainty of the $k_{obs}^{-1} - k_{12}^{-1}$ values.

not included in Figure 4 agree well with the calculated values except for the k_{obs} value at $\Delta G^0_{et} = -1.43$ eV, which is slightly larger than the calculated value (Figure 3). The calculated dependence of k_{obs} on ΔG^0_{et} (eq 13) predicts a decrease in the k_{obs} value from a diffusion-limited value with increasing the driving force of electron transfer ($-\Delta G^0_{et}$) when the k_{obs} values become smaller than the diffusion-limited value in the Marcus

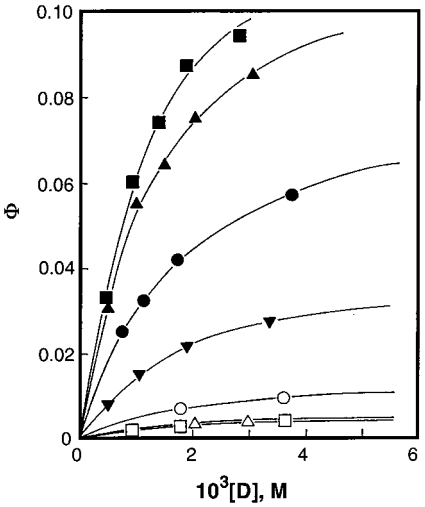

Figure 5. Plots of Φ vs [D] for the photoreduction of $AcrH^+$ (3.1×10^{-4} M) by the organometallic donors $CH_2{=}CHCH_2SiMe_3$ (△), $Me_2C{=}CHCH_2SiMe_3$ (□), $PhCH_2SiMe_3$ (○), $CH_2{=}CHCH_2SnPh_3$ (▼), $PhCH_2SnPh_3$ (●), $CH_2{=}CHCH_2SnBu_3$ (▲), and $Me_2C{=}CHCH_2SnBu_3$ (■) in deaerated MeCN at 298 K.

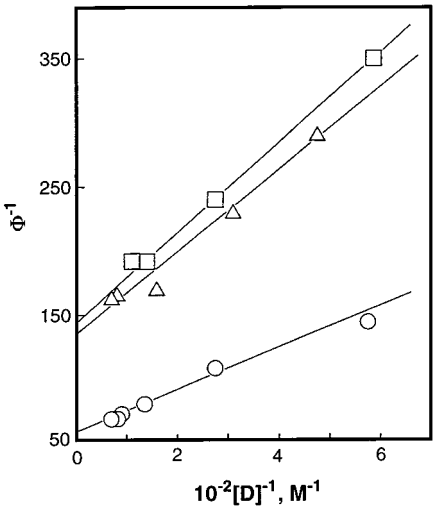

Figure 6. Plots of Φ^{-1} vs $[D]^{-1}$ for the photoreduction of $AcrH^+$ (3.1×10^{-4} M) by the organometallic donors $CH_2{=}CHCH_2SiMe_3$ (△), $Me_2C{=}CHCH_2SiMe_3$ (□), and $PhCH_2SiMe_3$ (○) in deaerated MeCN at 298 K.

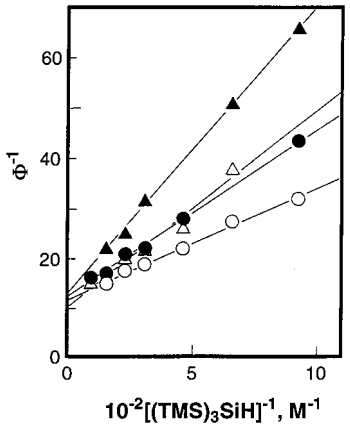

Figure 7. Plots of Φ^{-1} vs $[(TMS)_3SiH]^{-1}$ for the photoreduction of $AcrH^+$ (2.9×10^{-4} M; ○), QuH^+ (6.0×10^{-4} M; ●), 2-$MeQuH^+$ (6.0×10^{-4} M; △), and 4-$MeQuH^+$ (6.0×10^{-4} M; ▲) by $(TMS)_3SiH$ in deaerated MeCN at 298 K.

inverted region ($\Delta G^0_{et} < -\lambda$), provided that the λ value is constant in a series of electron transfer reactions.[38] The absence of a Marcus inverted region has well been recognized in forward photoinduced electron transfer reactions.[35] In the case of back electron transfer reactions, however, the observation of the Marcus-inverted region has been well established.[41,42] The absence of an inverted region in forward photoinduced electron transfer reactions in the highly exergonic region ($\Delta G^0_{et} < -\lambda$) is explained by an increase in the λ value from the value for a contact radical ion pair (CRIP) or a solvent separated radical ion pair (SSRIP) which has a larger distance between the radical ions in the highly exergonic region.[41d,43] In the case of back electron transfer reactions, electron transfer may occur in CRIP as is discussed later.

Quantum Yields. The quantum yields (Φ) of the photoaddition reactions of organometallic compounds with $AcrH^+$ were determined from the spectral change under irradiation of monochromatized light of $\lambda = 358$ nm (see the Experimental Section). The Φ values increase with an increase in the concentration of the organometallic compound [D], to approach a limiting value (Φ_∞) in accordance with eq 14 as shown in Figure 5. Equation 14 is rewritten by eq 15, and the linear plots of Φ^{-1} and $[D]^{-1}$ are shown in Figure 6. From slopes and

$$\Phi = \Phi_\infty K_{obs}[D]/(1 + K_{obs}[D]) \quad (14)$$

$$\Phi^{-1} = \Phi_\infty{}^{-1}[1 + (K_{obs}[D])^{-1}] \quad (15)$$

intercepts are obtained the Φ_∞ and K_{obs} values. The K_{obs} values can be converted to the corresponding rate constants (k_{obs}) provided that the excited state of $AcrH^+$ involved in the photochemical reaction is singlet ($AcrH^+$*; $k_{obs} = K_{obs}\tau^{-1}$, $\tau =$ 37 ns). The k_{obs} values were also obtained for the photoreduction of X-QuH^+ by $(TMS)_3SiH$ from the linear plots of Φ^{-1} and $[(TMS)_3SiH]^{-1}$ (Figure 7). The k_{obs} values are listed in Table 6, where the k_{obs} values agree well with the corresponding values determined independently by the fluorescence quenching. Such agreement strongly indicates that the photoreduction of $AcrH^+$ and X-QuH^+ by organosilanes and organostannanes proceeds via photoinduced electron transfer from these organometallic compounds to the singlet excited states, $AcrH^+$* and X-QuH^+*.

Regioreversal Addition via Photoinduced Electron Transfer. On the basis of the above results, the reaction mechanism for the photoaddition reactions of allylic silanes and stannanes with $AcrH^+$ is summarized as shown representatively for the photoaddition of $Me_2C{=}CHCH_2SnBu_3$ with $AcrH^+$ in Scheme 1. The reaction is initiated by photoinduced electron transfer (k_{obs}) from the allylic stannane to the singlet excited state (^{1}-$AcrH^+$*) to give the radical cation−acridinyl radical pair ($Me_2C{=}CHCH_2SnBu_3{}^{\bullet+}$ $AcrH^\bullet$). The metal−carbon bonds of radical cations of organostannanes and organosilanes are known to be cleaved to give the alkyl or allyl radicals.[15c,44−47] The bond cleavage has been shown to occur via an S_N2 reaction with a nucleophilic solvent such as MeCN (Scheme 1).[45−47] Thus, the radicals produced by the photoinduced electron transfer oxidation with $AcrH^+$* may be coupled within the cage to yield the adducts selectively without dimerization of free $AcrH^\bullet$ radicals escaped from the cage, in competition with the back electron transfer to the ground state (k_{bet}). A similar mechanism has been proposed by Mariano and co-workers for the photoaddition reaction of allylic silanes with pyrrolinium ions.[1,2] The identical regiochemical outcome in the photoaddition of 1,1- and 3,3-dimethylallyl silanes to give the same adduct indicates that the free allyl radical produced by desilylation of the organosilane radical cation is responsible for the product formation step rather than the carbon−carbon bond formation between the organosilane radical cation and pyrrolidinyl radical.[1,2] If the free allyl

SCHEME 1

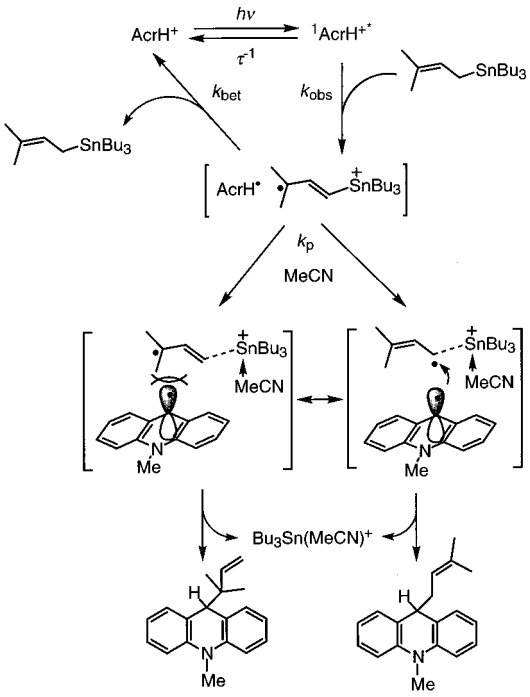

radicals are responsible for the product formation step in the photoaddition reactions with $AcrH^+$, the regioselectivity would be independent of the metal moieties. Although the regioselectivity of the photoaddition of prenylsilane with $AcrH^+$ is the same as that of the photoaddition with the pyrrolinium ion (i.e., the selective formation of γ-adduct, eq 2), the different regioselectivities are obtained in the case of the photoaddition of unsymmetrical allylic stannanes (Table 1). Moreover, the ratios of the yields of the α to γ adducts vary depending on the substituents of allylic stannanes (Table 1).[48] Thus, the C−C bond formation may occur in the cage in which the trialkylmetal ion exists in proximity of $AcrH^•$, affecting the regioselectivity for the C−C bond formation with the prenyl radical (Scheme 1). If the back electron transfer occurs in the cage as shown in Scheme 1, the decay of $AcrH^•$ in the radical pair should follow first-order kinetics rather than second-order kinetics for the out-of-cage radicals. This was confirmed by the laser-flash experiments (vide infra).

The direct observation of the radical pair of $AcrH^•$ in Scheme 1 has been hampered because of the strong fluorescence of $AcrH^+$ exhibiting a negative absorption at 488 nm in which the transient absorption spectrum of $AcrH^•$ should be observed.[49] Thus, the back electron transfer in Scheme 1 should be sufficiently slow to be able to detect $AcrH^•$ produced in the photoinduced electron transfer reactions from organosilanes and organostannanes to $AcrH^{+}$*. Laser-flash irradiation (355 nm from a Nd:YAG laser) of $AcrH^+$ (5.0×10^{-5} M) in a deaerated MeCN solution containing $CH_2{=}CHCH_2SiMe_3$ and $PhCH_2SiMe_3$ gave a transient absorption band at $\lambda_{max} = 500$ nm because of $AcrH^•$,[49] as is shown in Figure 8a,b, respectively. The absorption band due to $PhCH_2SiMe_3^{•+}$ ($\lambda_{max} = 530$ nm)[47] is overlapped in Figure 8b. The formation of $AcrH^•$ in photoinduced electron transfer from $PhCH_2SiMe_3$ to $AcrH^{+}$* is also confirmed by the ESR spectrum measured under irradiation of a frozen MeCN solution containing $PhCH_2SiMe_3$ and $AcrH^+$ with a high-pressure mercury lamp at 143 K (Figure 9).[50] The same ESR spectrum with the g value of 2.0032 was obtained by photoirradiation of an MeCN solution containing an electron donor (ferrocene) and $AcrH^+$.[51,52] Thus, the observed

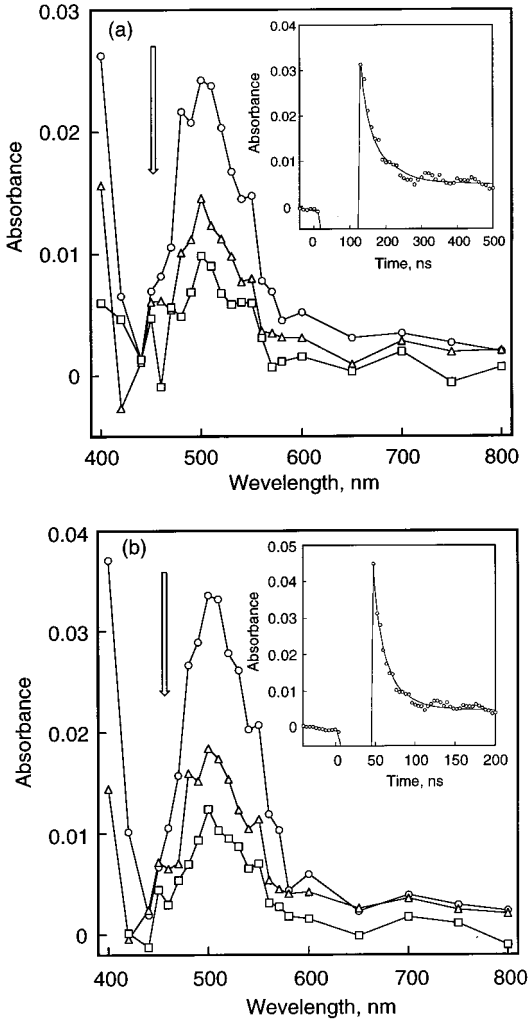

Figure 8. Transient absorption spectra observed in the photoreduction of $AcrH^+$ (1.7×10^{-4} M) with (a) $CH_2{=}CHCH_2SiMe_3$ (2.8×10^{-2} M) at 160 (○), 200 (△) and 650 ns (□) and (b) $PhCH_2SiMe_3$ (2.8×10^{-2} M) at 50 (○), 70 (△), and 100 ns (□) after laser excitation in deaerated MeCN at 298 K. Inset: Kinetic trace for $AcrH^•$ produced in the photoinduced electron transfer reactions from (a) $CH_2{=}CHCH_2SiMe_3$ and (b) $PhCH_2SiMe_3$ to $AcrH^{+}$* at $\lambda = 500$ nm after laser excitation in deaerated MeCN at 298 K.

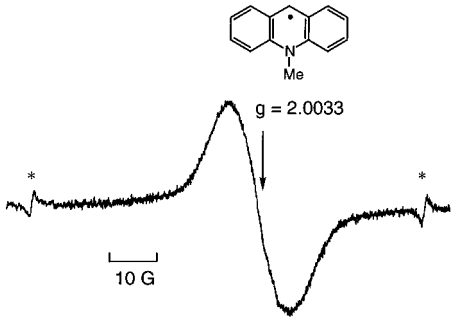

Figure 9. ESR spectrum of frozen MeCN containing $AcrH^+ClO_4^-$ (1.0×10^{-2} M) and $PhCH_2SiMe_3$ (5.0×10^{-2} M) with a high-pressure mercury lamp at 143 K. The asterisk (*) denotes an Mn^{2+} ESR marker.

ESR signal in Figure 9 is assigned to $AcrH^•$ produced by photoinduced electron transfer from $PhCH_2SiMe_3$ to $AcrH^{+}$*.

The absorption at $\lambda = 500$ nm decays obeying first-order kinetics, as is shown in the insets of Figure 8 as expected for the back electron transfer within the cage (Scheme 1). Thus, the decay rate of the radical pair corresponds to the back electron transfer to the ground state (k_{bet}) and the bond-cleavage process

SCHEME 2

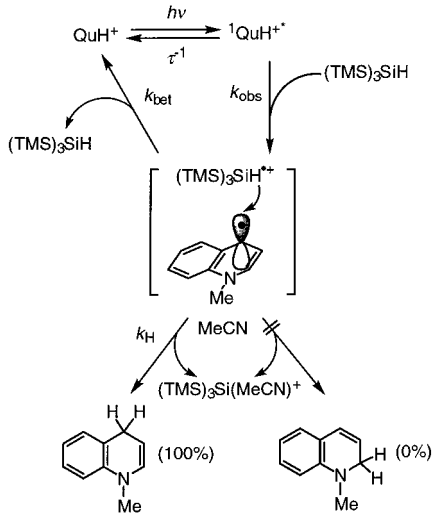

(k_p) to yield the product. Because $k_{bet} \gg k_p$ (i.e., $\Phi_\infty \ll 1$ in eq 18), the first-order decay rates in insets of Figure 8a,b correspond mainly to the back electron transfer from AcrH$^\bullet$ to $CH_2{=}CHCH_2SiMe_3^{\bullet+}$ ($k_{bet} = 2.9 \times 10^7\ s^{-1}$) and $PhCH_2SiMe_3^{\bullet+}$ ($k_{bet} = 7.9 \times 10^7\ s^{-1}$), respectively.[53] From eq 12 is derived the reorganization energy of back electron transfer as given by eq 16:

$$\lambda = 2[-kT\ln(hk_{bet}/kT)] - \Delta G^0_{et} - [(\Delta G^0_{et} - 2[-kT\ln(hk_{bet}/kT)])^2 - (\Delta G^0_{et})^2]^{1/2} \quad (16)$$

The λ values for the back electron transfer from AcrH$^\bullet$ to $CH_2{=}CHCH_2SiMe_3^{\bullet+}$ and $PhCH_2SiMe_3^{\bullet+}$ are obtained from the k_{bet} values using eq 16 as 0.80 and 0.89 eV, respectively.[54] The λ values thus determined agree with the averaged λ value (0.90 eV) for forward photoinduced electron transfer from organosilanes and organostannanes (Figure 4).

In accordance with Scheme 1, the quantum yield is expressed by eq 17, which agrees well with the experimental result (eq 14).

$$\Phi = [k_p k_{obs}\tau/(k_p + k_{bet})][D]/(1 + k_{obs}\tau[D]) \quad (17)$$

The limiting quantum yield Φ_∞ is then expressed by eq 18:

$$\Phi_\infty = k_p/(k_p + k_{bet}) \quad (18)$$

where the competition between the rates of bond-cleavage of the organometallic radical cation (k_p) and the back electron transfer (k_{bet}) determines the limiting quantum yield. Thus, the small Φ_∞ values of organosilanes as compared to those of the organostannane counterparts shown in Table 6 may well be ascribed to the stronger Si−C bonds than the Sn−C bonds.[50] The faster back electron transfer from AcrH$^\bullet$ to organosilane radical cations as expected from the more favorable energetics judging from the higher oxidation potentials of organosilanes than those of organostannane counterparts may also contribute the smaller Φ_∞ values.

The photoreduction of X-QuH$^+$ by $(TMS)_3SiH$ may also occur via photoinduced electron transfer from $(TMS)_3SiH$ to ^{1}X-QuH^{+}* as shown representatively for the reaction between $(TMS)_3SiH$ and QuH$^+$ in Scheme 2. The reaction is initiated by photoinduced electron transfer from $(TMS)_3SiH$ to ^{1}QuH^{+}* to give the metal hydride radical cation−quinolinyl radical pair, followed by the hydrogen transfer in the cage, in competition with the back electron transfer to the reactant pair, to yield the hydride adduct selectively without dimerization of free QuH$^\bullet$ radicals escaped from the cage.

In accordance with Scheme 2, the dependence of Φ on the $(TMS)_3SiH$ concentration may be expressed by eq 19:

$$\Phi = [k_H k_{obs}\tau/(k_H + k_{bet})][(TMS)_3SiH]/(1 + k_{obs}\tau[(TMS)_3SiH]) \quad (19)$$

where k_{obs} and k_{bet} are the rate constants of photoinduced electron transfer and the back electron transfer, respectively, τ is the lifetime of ^{1}X-QuH^{+}*, and k_H is the rate constant of hydrogen transfer from $(TMS)_3SiH^{\bullet+}$ to X-QuH$^\bullet$. The existence of a rate-determining hydrogen transfer step following the photoinduced electron transfer in Scheme 2 is confirmed by the deuterium isotope effect determined as $\Phi_H/\Phi_D = 1.9$ (in Table 6) from the ratio of the limiting quantum yields Φ_∞ of $(TMS)_3SiH$ and $(TMS)_3SiD$, which corresponds to $(k_H/k_D)[(k_D + k_{bet})/(k_H + k_{bet})]$ in eq 19. In contrast, no kinetic isotope effect has been observed in the k_{obs} values (Table 6). Similar Φ_∞ values irrespective of methyl substituents in Table 6 show sharp contrast with the diminished reactivity of 2-MeQuH$^+$ in the thermal reduction by Bu_3SnH (eq 6). Thus, the thermal reduction of X-QuH$^+$ by Bu_3SnH may proceed via a polar mechanism exhibiting the significant steric effect of the methyl group at the C-2 carbon where the C−H bond is formed with X-QuH$^+$. In contrast, no significant steric effect has been observed in the photochemical reactions via the photoinduced electron transfer. The spin density of QuH$^\bullet$ with the optimized geometry is calculated using density functional theory at the Becke3LYP/6-31+G* level (see the Experimental Section).[26,27] Because the spin density of QuH$^\bullet$ is greatest at the C-4 position (0.54) as compared to the value at the C-2 position (0.39), the hydrogen transfer from the metal hydride radical cation to QuH$^\bullet$ occurs at the C-4 position to yield the corresponding 1,4-isomer exclusively.[55] In contrast to the spin density, the MP2/6-31++G* calculation indicates that the charge density of QuH$^+$ is greatest at the C-2 position (0.16) as compared to the value at the C-4 position (0.003).[56] Thus, the nucleophilic attack of Bu_3SnH occurs at the C-2 position to yield the corresponding 1,2-isomer selectively.

In conclusion, the photoinduced electron transfer from organosilanes and organostannanes to AcrH^{+}* and X-QuH^{+}* provides a unique reaction pathway for regioselective addition of organosilanes and organostannanes, which is reversed in the corresponding thermal nucleophilic addition reactions with AcrH$^+$ and X-QuH$^+$.

Acknowledgment. This work was partially supported by a Grant-in-Aid for Scientific Research Priority Area (No. 11228205) from the Ministry of Education, Science, Culture and Sports, Japan.

References and Notes

(1) (a) Mariano, P. S. In *Photoinduced Electron Transfer*; Fox, M. A., Chanon, M., Eds.; Elsevier: Amsterdam, The Netherlands, 1988; Part C, p 372. (b) Mariano, P. S. *Acc. Chem. Res.* **1983**, *16*, 130. (c) Mariano, P. S. In *Synthetic Organic Chemistry*; Horspool, W. M., Ed.; Plenum Press: London, 1984.

(2) (a) Ohga, K.; Mariano, P. S. *J. Am. Chem. Soc.* **1982**, *104*, 617. (b) Ohga, K.; Yoon, U. C.; Mariano, P. S. *J. Org. Chem.* **1984**, *49*, 213. (c) Cho, I.-S.; Tu, C.-L.; Mariano, P. S. *J. Am. Chem. Soc.* **1990**, *112*, 3594. (d) Su, Z.; Mariano, P. S.; Falvey, D. E.; Yoon, U. C.; Oh, S. W. *J. Am. Chem. Soc.* **1998**, *120*, 10676. (e) Takahashi, Y.; Miyashi, T.; Yoon, U. C.; Oh, S. W.; Mancheno, M.; Su, Z.; Falvey, D. F.; Mariano, P. S. *J. Am. Chem. Soc.* **1999**, *121*, 3926.

(3) (a) Mattes, S. L.; Farid, S. *Acc. Chem. Res.* **1982**, *15*, 80. (b) Eaton, D. F. *J. Am. Chem. Soc.* **1980**, *102*, 3278, 3280. (c) Lan, J. Y.; Schuster,

G. B. In *Advances in Electron-Transfer Chemistry*; Mariano, P. S., Ed.; JAI Press: Greenwich, CT, 1991; Vol. 1.

(4) (a) Fukuzumi, S. In *Electron Transfer in Chemistry*; Balzani, V., Ed.; Wiley-VCH: Weinheim, Germany, 2001; Vol. 5, in press. (b) Fukuzumi, S. *Bull. Chem. Soc. Jpn.* **1997**, *70*, 1. (c) Fukuzumi, S.; Itoh, S. In *Advances in Photochemistry*; Neckers, D. C., Volman, D. H., von Bünau, G., Eds.; Wiley: New York, 1998; Vol. 25, pp 107−172.

(5) (a) Sakurai, H.; Sakamoto, K.; Kira, M. *Chem. Lett.* **1984**, 1213. (b) Nakadaira, Y.; Komatsu, N.; Sakurai, H. *Chem. Lett.* **1985**, 1781. (c) Mizuno, K.; Ikeda, M.; Otsuji, Y. *Tetrahedron Lett.* **1985**, *26*, 461. (d) Mizuno, K.; Kobata, T.; Maeda, R.; Otsuji, Y. *Chem. Lett.* **1990**, 1821. (e) Fukuzumi, S.; Kitano, T.; Mochida, K. *Chem. Lett.* **1989**, 2177. (f) Fukuzumi, S.; Kitano, T.; Mochida, K. *Chem. Lett.* **1990**, 1774. (g) Fukuzumi, S.; Kitano, T.; Mochida, K. *J. Chem. Soc., Chem. Commun.* **1990**, 1236.

(6) (a) Fukuzumi, S.; Fujita, M.; Otera, J.; Fujita, Y. *J. Am. Chem. Soc.* **1992**, *114*, 10271. (b) Fukuzumi, S.; Okamoto, T.; Otera, J. *J. Am. Chem. Soc.* **1994**, *116*, 5503. (c) Mikami, K.; Matsumoto, S.; Ishida, A.; Takamuku, S.; Suenobu, T.; Fukuzumi, S. *J. Am. Chem. Soc.* **1995**, *117*, 11134. (d) Mikami, K.; Matsumoto, S.; Okubo, Y.; Fujitsuka, M.; Ito, O.; Suenobu, T.; Fukuzumi, S. *J. Am. Chem. Soc.* **2000**, *122*, 2236.

(7) (a) Yamamoto, H. *Lewis Acid Chemistry: A Practical Approach*; Oxford University Press: Oxford, U.K., 1999. (b) *Selectivities in Lewis Acid Promoted Reactions*; Schinzer, D., Ed.; Kluwer Academic Publishers: Dordrecht, The Netherlands, 1989. (c) Santelli, M.; Pons, J.-M. *Lewis Acids and Selectivity in Organic Synthesis*; CRC Press: Boca Raton, FL, 1995.

(8) (a) Colvin, E. W. *Silicon in Organic Synthesis*; Butterworth: London, 1981. (b) Mukaiyama, T. *Angew. Chem., Int. Ed. Engl.* **1977**, *16*, 817. (c) Mukaiyama, T.; Murakami, M. *Synthesis* **1987**, 1043. (d) Gennari, C. In *Selectivities in Lewis Acid Promoted Reactions*; Schinzer, D., Ed.; Kluwer Academic Publ.: Dordrecht, The Netherlands, 1989; Chapter 4, p 53. (e) Heathcock, C. H. *Aldrichimica Acta* **1990**, *23*, 99. (f) Hosomi, A. *Acc. Chem. Res.* **1988**, *21*, 200.

(9) (a) Yamamoto, Y. *Acc. Chem. Res.* **1987**, *20*, 243. (b) Naruta, Y. *J. Am. Chem. Soc.* **1980**, *102*, 3774.

(10) (a) Davies, A. G. *Organotin Chemistry*; VCH: Weinheim, Germany, 1997; p 327. (b) Smith, P. J., Ed. *Chemistry of Tin*, 2nd ed.; Blackie: London, 1997; p 578.

(11) (a) Kursanov, D. N.; Parnes, Z. N.; Loim, N. M. *Synthesis* **1974**, 633. (b) Weber, W. P. *Silicon Reagents for Organic Synthesis*; Springer-Verlag: London, 1983. (c) Corey, J. Y.; Braddock-Wilking, J. *Chem. Rev.* **1999**, *99*, 175.

(12) (a) Neumann, W. P. *Synthesis* **1987**, 665. (b) Curran, D. P. *Synthesis* **1988**, 417. (c) Jasperse, C. P.; Curran, D. P.; Fevig, T. L. *Chem. Rev.* **1991**, *91*, 1237. (d) Giese, B. *Radicals in Organic Synthesis: Formation of Carbon−Carbon Bonds*; Pergamon Press: Oxford, U.K., 1986. (d) Ryu, I.; Sonoda, N.; Curran, D. P. *Chem. Rev.* **1996**, *96*, 177. (e) Chatgilialoglu, C.; Crich, D.; Komatsu, M.; Ryu, I. *Chem. Rev.* **1999**, *99*, 1991.

(13) Chatgilialoglu, C. *Acc. Chem. Res.* **1992**, *25*, 188.

(14) (a) Kochi, J. K. *Organometallic Mechanisms and Catalysis*; Academic Press: New York, 1978; p 501. (b) Klingler, R. J.; Mochida, K.; Kochi, J. K. *J. Am. Chem. Soc.* **1979**, *101*, 6626. (c) Yang, D.; Tanner, D. D. *J. Org. Chem.* **1986**, *51*, 2267.

(15) (a) Stout, D. M.; Meyer, A. I. *Chem. Rev.* **1982**, *82*, 223. (b) Fukuzumi, S.; Tanaka, T. In *Photoinduced Electron Transfer*; Fox, M. A., Chanon, M., Eds.; Elsevier: Amsterdam, The Netherlands, 1988; Part C, p 578. (c) Fukuzumi, S. In *Advances in Electron-Transfer Chemistry*; Mariano, P. S., Ed.; JAI Press: Greenwich, CT, 1992; Vol. 2, p 65.

(16) (a) Franke, M.; Steckhan, E. *Angew. Chem., Int. Ed. Engl.* **1988**, *27*, 265. (b) Westerhausen, D.; Herrmann, S.; Hummel, W.; Steckhan, E. *Angew. Chem., Int. Ed. Engl.* **1992**, *31*, 1529. (c) Ishitani, O.; Inoue, N.; Koike, K.; Ibusuki, T. *J. Chem. Soc., Chem. Commun.* **1994**, 367.

(17) A preliminary report has appeared: Fukuzumi, S.; Fujita, M.; Otera, J. *J. Chem. Soc., Chem. Commun.* **1993**, 1536.

(18) Roberts, R. M. G.; Ostović, D.; Kreevoy, M. M. *Faraday Discuss. Chem. Soc.* **1982**, *74*, 257.

(19) Fukuzumi, S.; Koumitsu, S.; Hironaka, K.; Tanaka, T. *J. Am. Chem. Soc.* **1987**, *109*, 305.

(20) Hosomi, A.; Shirahata, A.; Sakurai, H. *Chem. Lett.* **1978**, 901.

(21) Fukuzumi, S.; Tokuda, Y.; Kitano, T.; Okamoto, T.; Otera, J. *J. Am. Chem. Soc.* **1993**, *115*, 8960.

(22) Perrin, D. D.; Armarego, W. L. F. *Purification of Laboratory Chemicals*; Butterworth-Heinemann: Oxford, U.K., 1988.

(23) (a) Ishikawa, K.; Fukuzumi, S.; Goto, T.; Tanaka, T. *J. Am. Chem. Soc.* **1990**, *112*, 1578. (b) Fukuzumi, S.; Ishikawa, K.; Hironaka, K.; Tanaka, T. *J. Chem. Soc., Perkin Trans. 2* **1987**, 751.

(24) (a) Hatchard, C. G.; Parker, C. A. *Proc. R. Soc. London, Ser. A* **1956**, *235*, 518. (b) Calvert, J. C.; Pitts, J. N. *Photochemistry*; Wiley: New York, 1966; p 783.

(25) Sterwart, J. J. P. *J. Comput. Chem.* **1989**, *10*, 209; 221.

(26) (a) Becke, A. D. *J. Chem. Phys.* **1993**, *98*, 5648. (b) Lee, C.; Yang, W.; Parr, R. G. *Phys. Rev. B* **1988**, *37*, 785.

(27) Hehre, W. J.; Radom, L.; Schleyer, P. v. R.; Pople, J. A. *Ab Initio Molecular Orbital Theory*; Wiley: New York, 1986.

(28) Frisch, M. J.; Trucks, G. W.; Schlegel, H. B.; Scuseria, G. E.; Robb, M. A.; Cheeseman, J. R.; Zakrzewski, V. G.; Montgomery, J. A., Jr.; Stratmann, R. E.; Burant, J. C.; Dapprich, S.; Millam, J. M.; Daniels, A. D.; Kudin, K. N.; Strain, M. C.; Farkas, O.; Tomasi, J.; Barone, V.; Cossi, M.; Cammi, R.; Mennucci, B.; Pomelli, C.; Adamo, C.; Clifford, S.; Ochterski, J.; Petersson, G. A.; Ayala, P. Y.; Cui, Q.; Morokuma, K.; Malick, D. K.; Rabuck, A. D.; Raghavachari, K.; Foresman, J. B.; Cioslowski, J.; Ortiz, J. V.; Baboul, A. G.; Stefanov, B. B.; Liu, G.; Liashenko, A.; Piskorz, P.; Komaromi, I.; Gomperts, R.; Martin, R. L.; Fox, D. J.; Keith, T.; Al-Laham, M. A.; Peng, C. Y.; Nanayakkara, A.; Gonzalez, C.; Challacombe, M.; Gill, P. M. W.; Johnson, B.; Chen, W.; Wong, M. W.; Andres, J. L.; Gonzalez, C.; Head-Gordon, M.; Replogle, E. S.; Pople, J. A. *Gaussian 98*, Revision A.7; Gaussian, Inc.; Pittsburgh, PA, 1998.

(29) Fukuzumi, S.; Kuroda, S.; Tanaka, T. *J. Chem. Soc., Chem. Commun.* **1987**, 120.

(30) (a) Roberts, R. M. G.; Ostović, D.; Kreevoy, M. M. *J. Org. Chem.* **1983**, *48*, 2053. (b) Romoff, T. T.; Sampson, N. S.; van Eikeren, P. *J. Org. Chem.* **1987**, *52*, 4454. (c) Kim, D.; Lee, I.-S. H.; Kreevoy, M. M. *J. Am. Chem. Soc.* **1990**, *112*, 1889.

(31) (a) Fujita, M.; Hiyama, T. *J. Org. Chem.* **1988**, *53*, 5405. (b) Corriu, R. J. P.; Perz, R.; Reye, C. *Tetrahedron* **1983**, *39*, 999. (c) Fujita, M.; Hiyama, T. *J. Am. Chem. Soc.* **1984**, *106*, 4629. (d) Fujita, M.; Hiyama, T. *J. Am. Chem. Soc.* **1985**, *107*, 8294.

(32) (a) Fujita, M.; Ishida, A.; Takamuku, S.; Fukuzumi, S. *J. Am. Chem. Soc.* **1996**, *118*, 8566. (b) Fujita, M.; Fukuzumi, S. *J. Chem. Soc., Perkin Trans. 2* **1993**, 1915.

(33) Fukuzumi, S.; Noura, S. *J. Chem. Soc., Chem. Commun.* **1994**, 287.

(34) The one-electron reduction potentials of $AcrH^{+}$*, QuH^{+}*, 2-$MeQuH^{+}$*, and 4-$MeQuH^{+}$* were determined from the one-electron reduction potentials of the ground state[33] and the excitation energies, which are obtained from the frequencies of the absorption and emission maxima.[15b]

(35) (a) Rehm, A.; Weller, A. *Ber. Bunsen-Ges. Phys. Chem.* **1969**, *73*, 834. (b) Rehm, A.; Weller, A. *Isr. J. Chem.* **1970**, *8*, 259.

(36) When A* is replaced by A, eq 10 is also applied for thermal electron transfer reactions.

(37) In eq 10, the back electron transfer to the excited state is neglected when the back electron transfer to the ground state is much faster than the back electron transfer to the excited state.

(38) (a) Marcus, R. A. *Annu. Rev. Phys. Chem.* **1964**, *15*, 155. (b) Marcus, R. A. *J. Chem. Phys.* **1956**, *24*, 966. (c) Marcus, R. A. *Angew. Chem., Int. Ed. Engl.* **1993**, *32*, 1111.

(39) For nonadiabatic electron transfer, see: Marcus, R. A.; Sutin, N. *Biochim. Biophys. Acta* **1985**, *811*, 265.

(40) In eq 12, the work term of the product ions is neglected, because an electrostatic interaction in the radical ion pair is known to be small in a polar solvent such as MeCN.

(41) (a) Closs, G. L.; Miller, J. R. *Science* **1988**, *240*, 440. (b) Miller, J. R.; Calcaterra, L. T.; Closs, G. L. *J. Am. Chem. Soc.* **1984**, *106*, 3047. (c) Asahi, T.; Mataga, N. *J. Phys. Chem.* **1989**, *93*, 6575. (d) Gould, I. R.; Ege, D.; Moser, J. E.; Farid, S. *J. Am. Chem. Soc.* **1990**, *112*, 4290. (e) Gould, I. R.; Farid, S. *Acc. Chem. Res.* **1996**, *29*, 522.

(42) (a) McLendon, G. *Acc. Chem. Res.* **1988**, *21*, 160. (b) Winkler, J. R.; Gray, H. B. *Chem. Rev.* **1992**, *92*, 369. (c) McLendon, G.; Hake, R. *Chem. Rev.* **1992**, *92*, 481. (d) Mataga, N.; Miyasaka, H. In *Electron Transfer from Isolated Molecules to Biomolecules Part 2*; Jortner, J., Bixon, M., Eds.; Wiley: New York, 1999; p 431.

(43) (a) Rau, H.; Frank, R.; Greiner, G. *J. Phys. Chem.* **1986**, *90*, 2476. (b) Stevens, B.; Biver, C. J., III; McKeithan, D. N. *Chem. Phys. Lett.* **1991**, *187*, 590. (c) Kikuchi, K.; Takahashi, Y.; Katagiri, T.; Niwa, T.; Hoshi, M.; Miyashi, T. *Chem. Phys. Lett.* **1991**, *180*, 403.

(44) (a) Fukuzumi, S.; Mochida, K.; Kochi, J. K. *J. Am. Chem. Soc.* **1979**, *101*, 5961. (b) Fukuzumi, S.; Wong, C. L.; Kochi, J. K. *J. Am. Chem. Soc.* **1980**, *102*, 2928.

(45) Dinnocenzo, J. P.; Farid, S.; Goodman, J. L.; Gould, L. R.; Todd, W. P. *Mol. Cryst. Liq. Cryst.* **1991**, *194*, 151.

(46) (a) Cermenati, L.; Freccero, M.; Venturello, P.; Albini, A. *J. Am. Chem. Soc.* **1995**, *117*, 7869. (b) Dinnocenzo, J. P.; Farid, S.; Goodman, J. L.; Gould, I. R.; Todd, W. P.; Mattes, S. L. *J. Am. Chem. Soc.* **1989**, *111*, 8973.

(47) Dockery, K. P.; Dinnocenzo, J. P.; Farid, S.; Goodman, J. L.; Gould, I. R.; Todd, W. P. *J. Am. Chem. Soc.* **1997**, *119*, 1876.

(48) In the case of $Me_2C{=}CHCH_2Sn(cyclo\text{-}C_6H_{11})_3$, the *cyclo*-$C_6H_{11}$−Sn bond is also cleaved to give the adduct $AcrH(cyclo\text{-}C_6H_{11})$ (Table 1). However, cleavage of the $Me_2C{=}CHCH_2$−Sn bond is much more favored than cleavage of the *cyclo*-C_6H_{11}−Sn bond when the statistical factor is taken into account.

(49) (a) Peters, K. S.; Pang, E.; Rudzki, J. *J. Am. Chem. Soc.* **1982**, *104*, 5535. (b) Poulos, A. T.; Hammond, G. S.; Burton, M. E. *Photochem. Photobiol.* **1981**, *34*, 169.

(50) Butcher, E.; Rhodes, C. J.; Standing, M.; Davidson, R. S.; Bowser, R. *J. Chem. Soc., Perkin Trans. 2* **1992**, 1469.

(51) The ESR signal due to $PhCH_2SiMe_3^{\bullet+}$ may be overlapped with the $AcrH^{\bullet}$ signal, because the *g* value of $PhCH_2SiMe_3^{\bullet+}$ (2.003)[50] is nearly the same as the value of $AcrH^{\bullet}$. The detected radicals are stable after cutting off the light at 143 K. This indicates that an intermolecular electron transfer occurs after the photoinduced electron transfer from the organosilane to $AcrH^{+}$* to give the organosilane radical cation and $AcrH^{\bullet}$, which are separated with a long distance at 143 K, preventing the back electron transfer to the ground state.

(52) The ESR signal due to the ferricenium ion was too broad to be detected under the present experimental conditions.

(53) The k_{bet} value is apparently inconsistent with the large second-order rate constant of the Si−C bond cleavage of $PhCH_2SiMe_3^{\bullet+}$ with MeCN (3.2×10^9 M^{-1} s^{-1}) in dichloromethane, which leads to a short lifetime of the free radical cation ($PhCH_2SiMe_3^{\bullet+}$) in neat MeCN ($<10^{-9}$ s).[47] However, the Si−C bond cleavage rate of $PhCH_2SiMe_3^{\bullet+}$ in the cage (Scheme 1) may be much slower than the rate for the free radical cation to ensure the observed back electron transfer from $AcrH^{\bullet}$ to $PhCH_2SiMe_3^{\bullet+}$ in the cage, because the Si−C bond cleavage rate has been shown to be very sensitive to the steric nature of the alkyl substituents at silicon.[47]

(54) The ΔG^0_{bet} values of back electron transfer from $AcrH^{\bullet}$ to $CH_2{=}CHCH_2SiMe_3^{\bullet+}$ and $PhCH_2SiMe_3^{\bullet+}$ are −1.93 and −1.86 eV (obtained from the E^0_{ox} value of $AcrH^{\bullet}$ and the E^0_{ox} values of $CH_2{=}CHCH_2SiMe_3$ and $PhCH_2SiMe_3$),[6a,19] respectively, and these are in the Marcus inverted region ($\Delta G^0_{bet} < -\lambda$). The other solution of eq 16 gives a λ value in the normal region ($\Delta G^0_{bet} > -\lambda$), which is inconsistent with the results on the forward electron transfer reactions in Figure 3.

(55) In the photochemical reduction of QuH^+ by $(TMS)_3SiH$, no thermal isomerization of 1,4-QuH_2 to 1,2-QuH_2 was observed. The thermal isomerization rate is shown to be sensitive to the type of metal hydrides used as hydride donors (see Table 4).

(56) The semiempirical MNDO calculation gave a similar result: the charge density of QuH^+ is greatest at the C-2 position (0.18) as compared to the value at the C-4 position (0.098).